RSC Advances

ROYAL SOCIETY OF CHEMISTRY

PAPER

View Article Online
View Journal | View Issue

Cite this: *RSC Adv.*, 2021, **11**, 8033

N-type and p-type molecular doping on monolayer MoS_2†

Ong Kim Le,[ab] Viorel Chihaia,[c] Vo Van On[d] and Do Ngoc Son*[ab]

Monolayer MoS_2 has attracted much attention due to its high on/off current ratio, transparency, and suitability for optoelectronic devices. Surface doping by molecular adsorption has proven to be an effective method to facilitate the usage of MoS_2. However, there are no works available to systematically clarify the effects of the adsorption of F_4TCNQ, PTCDA, and tetracene on the electronic and optical properties of the material. Therefore, this work elucidated the problem by using density functional theory calculations. We found that the adsorption of F_4TCNQ and PTCDA turns MoS_2 into a p-type semiconductor, while the tetracene converts MoS_2 into an n-type semiconductor. The occurrence of a new energy level in the conduction band for F_4TCNQ and PTCDA and the valence band for tetracene reduces the bandgap of the monolayer MoS_2. Besides, the MoS_2/F_4TCNQ and MoS_2/PTCDA systems exhibit an auxiliary optical peak at the long wavelengths of 950 and 850 nm, respectively. Contrastingly, the MoS_2/tetracene modifies the optical spectrum of the monolayer MoS_2 only in the ultraviolet region. The findings are in good agreement with the experiments.

Received 29th November 2020
Accepted 15th February 2021

DOI: 10.1039/d0ra10075g

rsc.li/rsc-advances

1. Introduction

The monolayer MoS_2 is a semiconducting transition metal dichalcogenide with an optical bandgap of about 1.8 eV. This material has proven to possess high on/off current ratio and transparency, making it suitable for electronic and optoelectronic applications.[1,2] The properties of monolayer MoS_2 are adjustable by modifying the crystal structure, doping with different elements, and the adsorption of organic molecules.[3–6] The application of organic molecular adsorption is attractive because of advantages such as mechanical flexibility, easy fabrication, light weight, and low cost.[7,8] Organic molecular adsorption has been demonstrated as a viable method to optimize material properties,[6] also to protect MoS_2 from oxidation under ambient conditions.[9] Therefore, it is essential to understand the behavior of the organic adsorption on the monolayer MoS_2 to optimize its performance for optoelectronic uses.

Here, we studied the adsorption of three organic molecules, *i.e.*, 2,3,5,6-tetrafluoro-7,7,8,8-tetracyanoquinodimethane (F_4TCNQ), perylene-3,4,9,10-tetracarboxylic dianhydride (PTCDA), and tetracene. Where, F_4TCNQ is one of the most effective p-type dopants due to its strong ability of electron acceptance.[10–13] The experiment showed that F_4TCNQ could modify the electrical and optical properties of MoS_2.[11] Hu *et al.* confirmed that the deposition of F_4TCNQ on the monolayer MoS_2 allows convenient control of the radioactive exciton recombination for laser and LED applications.[12] The charge transfer within the F_4TCNQ–MoS_2 interface can tune electrical and gas sensing properties.[13] PTCDA and tetracene are popular organic semiconductors that have attracted many research interests in the past decades.[8,14–19] Tetracene was used for field-effect transistors.[20,21] The study of Habib showed the outstanding luminescent properties of the MoS_2/PTCDA system.[17] Also, Wang *et al.* have demonstrated the novel MoS_2/PTCDA hybrid heterojunction synapse transistor with both electrical and optical modulation and efficient gate tunability.[18] Besides, the MoS_2/tetracene is a good candidate for the anti-ambipolar field-effect transistor.[21]

The literature review showed that most of the available research is experiments, and there is no theoretical study available to elucidate the interaction between the MoS_2 monolayer and the mentioned organic molecules. Therefore, this work is going to clarify it by using the density functional theory (DFT) method and analyzing the electronic structure and optical properties of MoS_2 without and with the adsorption of F_4TCNQ, PTCDA, and tetracene. Furthermore, this work also considers the influences of pressure on the properties.

[a]*Ho Chi Minh City University of Technology (HCMUT), Ho Chi Minh City, Vietnam. E-mail: dnson@hcmut.edu.vn*

[b]*Vietnam National University, Ho Chi Minh City, Vietnam*

[c]*Institute of Physical Chemistry "Ilie Murgulescu" of the Romanian Academy, Splaiul Independentei 202, Sector 6, 060021 Bucharest, Romania*

[d]*Institute of Applied Technology, Thu Dau Mot University, No. 6 Tran Van On Street, Phu Hoa Ward, Thu Dau Mot City, Binh Duong Province 75000, Vietnam*

† Electronic supplementary information (ESI) available. See DOI: 10.1039/d0ra10075g

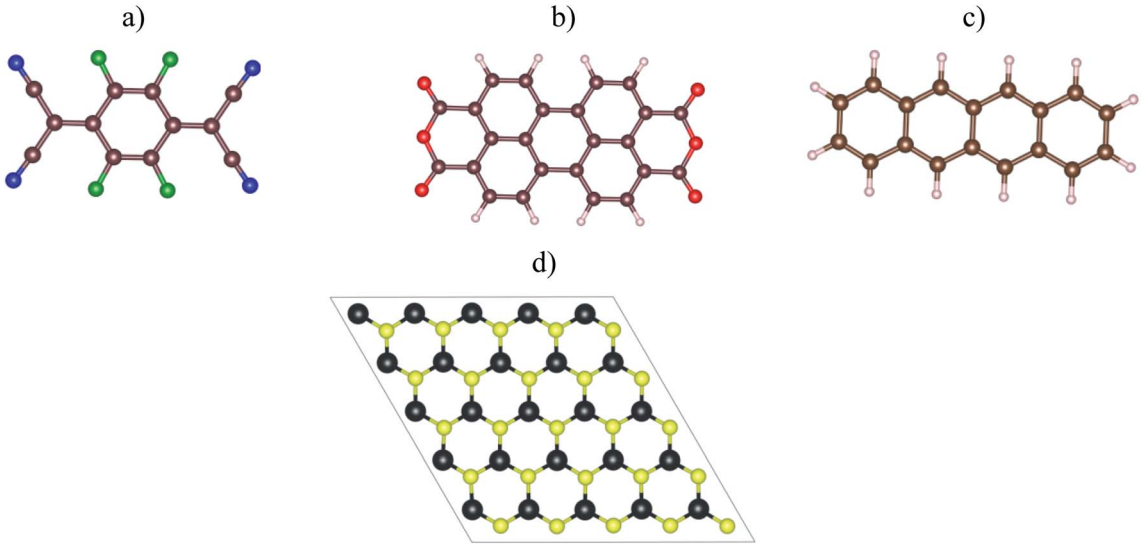

Fig. 1 The top view of organic molecules: (a) F_4TCNQ, (b) PTCDA, (c) tetracene, and (d) the monolayer MoS_2. Blue (N), green (F), brown (C), red (O), white (H), yellow (S), and black (Mo).

2. Computational method

Fig. 1a–c visualized the molecular structure of F_4TCNQ ($C_{12}F_4N_4$), PTCDA ($C_{24}H_8O_6$), and tetracene ($C_{18}H_{12}$), respectively. The monolayer MoS_2, shown in Fig. 1d, was described by a slab model with the 5×5 unit cell and a vacuum space of 27 Å along the normal direction of the MoS_2 surface.

The optimized geometry structure and total energy of the monolayer MoS_2 with organic molecular adsorption were obtained with the aid of the Vienna *ab initio* simulation package (VASP).[22–24] The projector-augmented-wave method was used to describe the valence electron–core ion interaction.[25,26] The electron exchange–correlation interactions were treated by using the PBE-GGA approximation of the Perdew–Burke–Ernzerhof,[27,28] which has shown to be a reasonable approximation for the bandgap of the monolayer MoS_2.[29] The plane-wave cutoff energy was 600 eV. The *k*-point mesh was sampled at $3 \times 3 \times 1$ in the first Brillouin zone by Monkhorst–Pack technique.[30] All atomic positions of MoS_2 and MoS_2/organic-molecule systems are fully relaxed during the geometry optimization until the interatomic forces meeting the upper criterion of 0.001 eV $Å^{-1}$.

The pressure applying to the system is defined by

$$P = \frac{E - E_0}{V - V_0}, \quad (1)$$

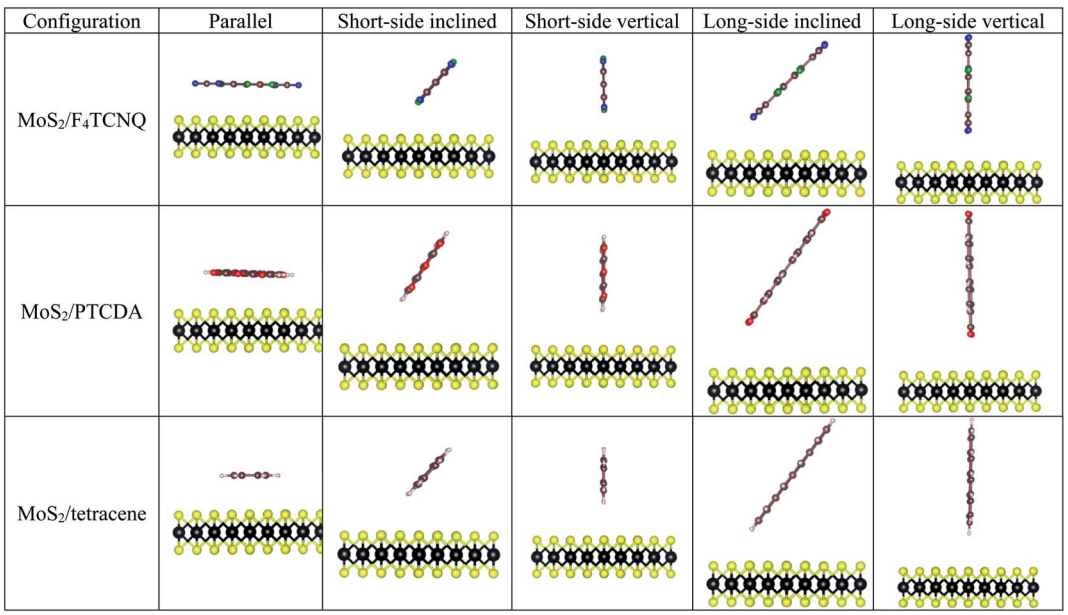

Fig. 2 The side view of the possible adsorption configurations of F_4TCNQ, PTCDA, and tetracene on the monolayer MoS_2.

Table 1 Adsorption energy E_a (eV) for different configurations on the monolayer MoS_2 without strain

Adsorption configuration	F_4TCNQ	PTCDA	Tetracene
Parallel	−0.009	0.019	0.039
Short-side inclined	**−0.055**	**−0.071**	**−0.046**
Short-side vertical	−0.038	−0.036	−0.030
Long-side inclined	−0.027	−0.031	−0.022
Long-side vertical	−0.023	−0.17	0.137

Table 2 Adsorption energy E_a and the shortest distance d from the organic molecule to the substrate surface

	MoS_2/F_4TCNQ		MoS_2/PTCDA		MoS_2/tetracene	
a^a (Å)	E_a (eV)	d (Å)	E_a (eV)	d (Å)	E_a (eV)	d (Å)
2.84	0.034	3.44	0.095	3.48	0.105	3.49
3.00	0.066	3.41	0.098	3.46	0.092	3.41
3.18	−0.009	3.47	0.019	3.53	0.039	3.49
3.32	−0.090	3.58	−0.019	3.60	−0.018	3.58
3.48	−0.130	3.60	−0.074	3.64	−0.128	3.61
3.64	−0.145	3.77	−0.080	3.79	−0.230	3.72

[a] 2.84 and 3.00 Å: for compressive pressure; 3.18 Å: without pressure; 3.32, 3.48, and 3.64 Å: for tensile strain.

where, the energy and volume of the strained (unstrained) system are denoted as E and V (E_0 and V_0), respectively. The volume of the unit cell of the monolayer MoS_2 is $V = \frac{\sqrt{3}}{2}a^2c$ (a is the lattice constant and c is the thickness of the slab). The pressure is modified by changing the lattice constant $a = b$.

The adsorption energy of F_4TCNQ, PTCDA, and tetracene on the monolayer MoS_2 is calculated by

$$E_a = E_{sub+om} - (E_{sub} + E_{om}), \quad (2)$$

where, E_{sub+om}, E_{sub}, and E_{om} are the total energy of the MoS_2/organic molecule system, the isolated monolayer MoS_2, and the isolated organic molecule, respectively.

The optical property of the systems was determined through the imaginary part $\varepsilon(\omega)$ of dielectric constant, which is calculated by the summation over empty states as follows:[31,32]

$$\varepsilon(\omega) = \frac{2\pi e^2}{V\varepsilon_0}\sum_{k,v,c}\left|\left\langle \xi_k^c|\hat{v}\cdot r|\xi_k^v\right\rangle\right|^2\delta\left[\hbar\omega - \left(E_k^v - E_k^c\right)\right], \quad (3)$$

here, ω is the frequency of emission, ε_0 is the dielectric constant of free space. The valence and conduction band wave functions are ξ_k^v and ξ_k^c, respectively. The unit cell volume is V, and the polarization vector of the electric field of the emission is $\hat{v}$.

3. Results and discussion

3.1. Structural properties

The optimized structural parameters for the monolayer MoS_2 were obtained in the previous publication,[33] where the optimized lattice constant was found to be $a = b = 3.18$ Å. To explore the adsorption properties of F_4TCNQ, PTCDA, and tetracene on the monolayer MoS_2, the geometry of the organic molecules with different configurations was optimized at several adsorption sites on the surface of MoS_2 as shown in Fig. 2. The most favorable adsorption of the F_4TCNQ, PTCDA, and tetracene molecules on the MoS_2 substrate was obtained for the short-side inclined configuration based on the most negative adsorption energy listed in Table 1.

Although the adsorption energy of the short-side inclined and parallel configurations are different, the electronic density of states (DOS) and the dielectric function are almost the same, as shown in Fig. S1 and S2 in the ESI.† Therefore, to make a comparison with the previous publication on polyethyleneimine,[33] we will perform a detailed analysis of the geometrical structure, the DOS, and the dielectric function for the parallel configuration of F_4TCNQ, PTCDA, and tetracene. Furthermore, we also found that the extension of the unit cell size to 6 × 6 and the inclusion of van der Waals correction (using vdW-DF functional) generated more negative adsorption energy (Tables S1 and S2†). However, the electronic structure of the MoS_2/F_4TCNQ, MoS_2/PTCDA, and MoS_2/tetracene systems remain the same as that of the unit cell 5 × 5 without van der Waals correction, as shown in Fig. S3.† Thus, it is acceptable to

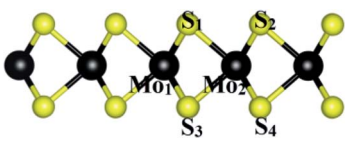

Fig. 4 The index of atoms for the bond lengths and angles.

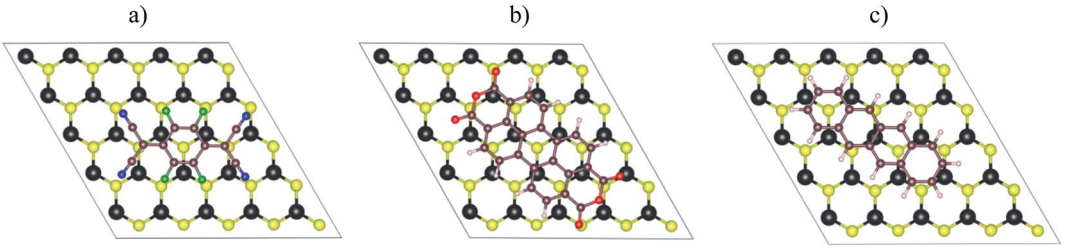

Fig. 3 The top view of the parallel adsorption configuration of the organic molecules on the monolayer MoS_2: (a) F_4TCNQ, (b) PTCDA, and (c) tetracene.

Table 3 Structural parameters of the MoS_2 substrate before and after the adsorption of the organic molecules. The index of atoms is described in Fig. 4

Parameters		MoS_2	MoS_2/F_4TCNQ	MoS_2/PTCDA	MoS_2/tetracene
Bonds (Å)	S_1–S_2	3.183	3.160	3.162	3.160
	S_1–S_3	3.126	3.144	3.146	3.132
	Mo_1–Mo_2	3.187	3.183	3.180	3.182
	Mo_2–S_1	2.415	2.415	2.415	2.413
Angles (°)	$Mo_1S_1Mo_2$	82.30	82.46	82.34	82.52
	$S_1Mo_2S_2$	82.30	81.76	81.88	81.84
	$S_1Mo_1S_3$	80.54	80.90	81.02	80.78

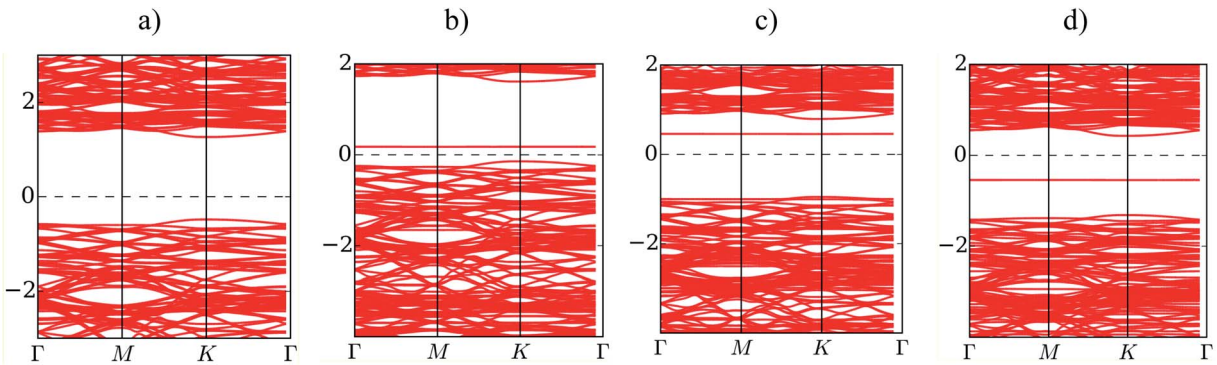

Fig. 5 The electronic band structure of (a) the monolayer MoS_2, (b) MoS_2/F_4TCNQ, (c) MoS_2/PTCDA, and (d) MoS_2/tetracene at zero pressure.

select the unit cell 5 × 5 and the PBE-GGA approximation in the present study.

Table 2 listed the adsorption energy and the vertical nearest distance to the MoS_2 surface of the F_4TCNQ, PTCDA, and tetracene molecules in the parallel configuration (Fig. 3). With the application of the tensile strain to the system, the organic molecules become stabilized with more negative adsorption energy relative to that at the lattice constant of 3.18 Å (without strain). The compressive pressure makes the molecules less stable with more positive adsorption energy. Table 2 also shows that the vertical nearest distance to the surface increases with the increase of the lattice constant. This result seems contradicted to the tendency of the more stable configuration of the adsorption upon modifying the tensile strain. Although the vertical nearest distance increases, the electrostatically attractive force between the adsorbates and MoS_2 increases at a faster rate.[33] Therefore, the adsorption energy becomes more negative. Besides, the interaction of the molecules with the surface is physisorption.

The geometrical parameters such as the bond length and bond angle of the MoS_2 substrate before and after the adsorption of the organic molecules are exhibited in Table 3. We found that the structural parameters did not change significantly after the adsorption of the molecules, which is consistent with the physical adsorption found in this work.

3.2. Electronic properties

Fig. 5 presents the band structure of MoS_2 before and after the adsorption of F_4TCNQ, PTCDA, and tetracene at zero pressure. The bandgap is determined by the difference between the conduction band minimum and the valence band maximum. We find that the isolated substrate shows a direct bandgap of 1.68 eV at the *K* point, as listed in Table 4. The calculated bandgap of 1.68 eV comes from the electronic contribution only, while the experimental value of 1.80 eV has included the exciton binding energy.[2,3,34] Upon the adsorption of the organic molecules, the new energy state occurs in the bandgap region of the MoS_2 substrate. The new energy level occurring above the Fermi level for the adsorption of F_4TCNQ and PTCDA implies that the substrate became the p-type semiconductor. Whilst, it occurring below the Fermi level for the adsorption of tetracene indicates that the monolayer MoS_2 became the n-type semiconductor. The existence of the new energy level shrinks the bandgap of the MoS_2 to 0.36, 1.43, and 0.72 eV for the

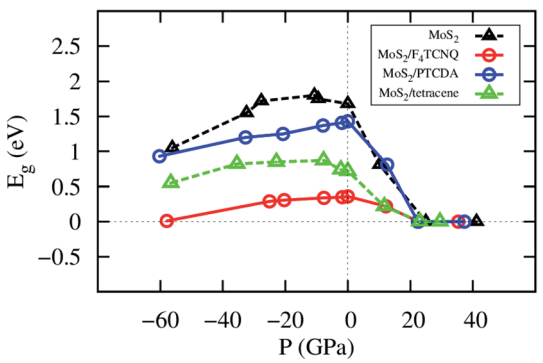

Fig. 6 The bandgap *versus* pressure of the monolayer MoS_2 with and without the adsorption of the organic molecules.

Table 4 The bandgap E_g of the monolayer MoS_2 with and without the adsorption of the organic molecules

	MoS_2[a]		MoS_2/F_4TCNQ		MoS_2/PTCDA		MoS_2/tetracene	
a (Å)	P (GPa)	E_g (eV)	P (GPa)	E_g (eV)	P (GPa)	E_g (eV)	P (GPa)	E_g (eV)
2.84	−56.18	1.05	−57.93	0.01	−60.27	0.93	−56.61	0.55
3.00	−32.44	1.55	−25.03	0.29	−32.70	1.20	−35.46	0.82
3.04	−27.65	1.72	−20.31	0.31	−20.74	1.25	−22.88	0.85
3.12	−10.69	1.80	−7.64	0.34	−7.93	1.37	−7.78	0.87
3.16	−9.46	1.75	−1.79	0.35	−1.91	1.41	−2.24	0.74
3.18	0	1.68	0	0.36	0	1.43	0	0.72
3.32	10.13	0.81	12.21	0.22	12.57	0.81	11.68	0.22
3.48	24.95	0	22.59	0	22.41	0	23.03	0
3.64	41.14	0	35.36	0	37.26	0	29.44	0

[a] In ref. 33.

adsorption of F_4TCNQ, PTCDA, and tetracene, respectively. However, the bandgap of the MoS_2 remains the direct bandgap nature after the adsorption of the organic molecules.

The change of the lattice constant modifies the pressure applied to the system. The details of the bandgap and the pressure are described in Table 4 and visualized in Fig. 6. We found that the bandgap behavior of MoS_2/tetracene is similar to that of the monolayer MoS_2, which exhibits a concave-downward curve with the maximum bandgap of 0.87 and 1.80 eV found at the pressure of −7.78 and −10.69 GPa for the MoS_2/tetracene and monolayer MoS_2, respectively. The concave-downward curve for the bandgap *versus* the pressure for the MoS_2 system was found to be in good agreement with experiment,[35] while that for the MoS_2/tetracene is similar to that of an n-type semiconductor, the MoS_2/PEI interface, in the previous study.[33,36] There is a little difference in the behavior of the bandgap *versus* the pressure for MoS_2/F_4TCNQ and MoS_2/PTCDA compared to that of the monolayer MoS_2. That is the bandgap somehow linearly increases to a maximum value and then decreases with more positive pressures. The maximum value is 0.36 and 1.43 eV at the zero pressure for MoS_2/F_4TCNQ and MoS_2/PTCDA, respectively. We have to impress that MoS_2/F_4TCNQ and MoS_2/PTCDA are the p-type semiconductors, which are different from the n-type of the MoS_2/tetracene. The monolayer MoS_2, MoS_2/F_4TCNQ, MoS_2/PTCDA, and MoS_2/tetracene were found to be completely converted to the metal with the bandgap of 0 eV at the pressure of 24.95, 22.59, 22.41, and 23.03 GPa, respectively.

Table 5 The point charge (in the unit of e) of the MoS_2/F_4TCNQ, MoS_2/PTCDA, and MoS_2/tetracene systems

MoS_2/F_4TCNQ		
P (GPa)	MoS_2	F_4TCNQ
−57.93	−0.226	+0.226
−25.03	−0.098	+0.098
0	−0.073	+0.073
12.21	−0.144	+0.144
22.59	−0.231	+0.231
MoS_2/PTCDA		
P (GPa)	MoS_2	PTCDA
23.03	−0.015	+0.015
29.44	−0.017	+0.017
−20.74	−0.019	+0.019
0	−0.020	+0.020
12.57	−0.021	+0.021
22.41	−0.025	+0.025
MoS_2/tetracene		
P (GPa)	MoS_2	Tetracene
−56.61	+0.062	−0.062
−35.46	+0.060	−0.060
−22.88	+0.052	−0.052
−7.78	+0.045	−0.045
0	+0.048	−0.048
11.68	+0.050	−0.050
23.03	+0.103	−0.103
29.44	+0.363	−0.363

In a complex structure, the Bader point charge of an atom was determined in two steps: (1) calculating the charge by the Bader partition technique, and (2) subtracting the charge obtained in step (1) to that of the neutral atom. In the pseudopotential method of the DFT, one considers the contribution of valence electrons only. Table 5 presents the minus–plus signs as the loss and gain of charge, respectively. We found that F_4TCNQ and PTCDA accept while MoS_2 donates the charge. Contrastingly, the tetracene donates while MoS_2 gains the charge. These results are in a good correlation with the p-type doping nature of F_4TCNQ and PTCDA and the n-type doping of tetracene on the MoS_2 monolayer.

The electronic density of states (DOS) in Fig. 7a–c shows that the adsorption of F_4TCNQ, PTCDA, and tetracene contributes to the appearance of the new state coming from the p_z orbital of the organic molecules. As shown in Fig. 7d–f, the charge clouds of the atoms of the organic molecules clearly show the shape of p_z orbitals along the vertical direction, the vector **c**. The charge accumulation was found to more dominant on the F_4TCNQ and

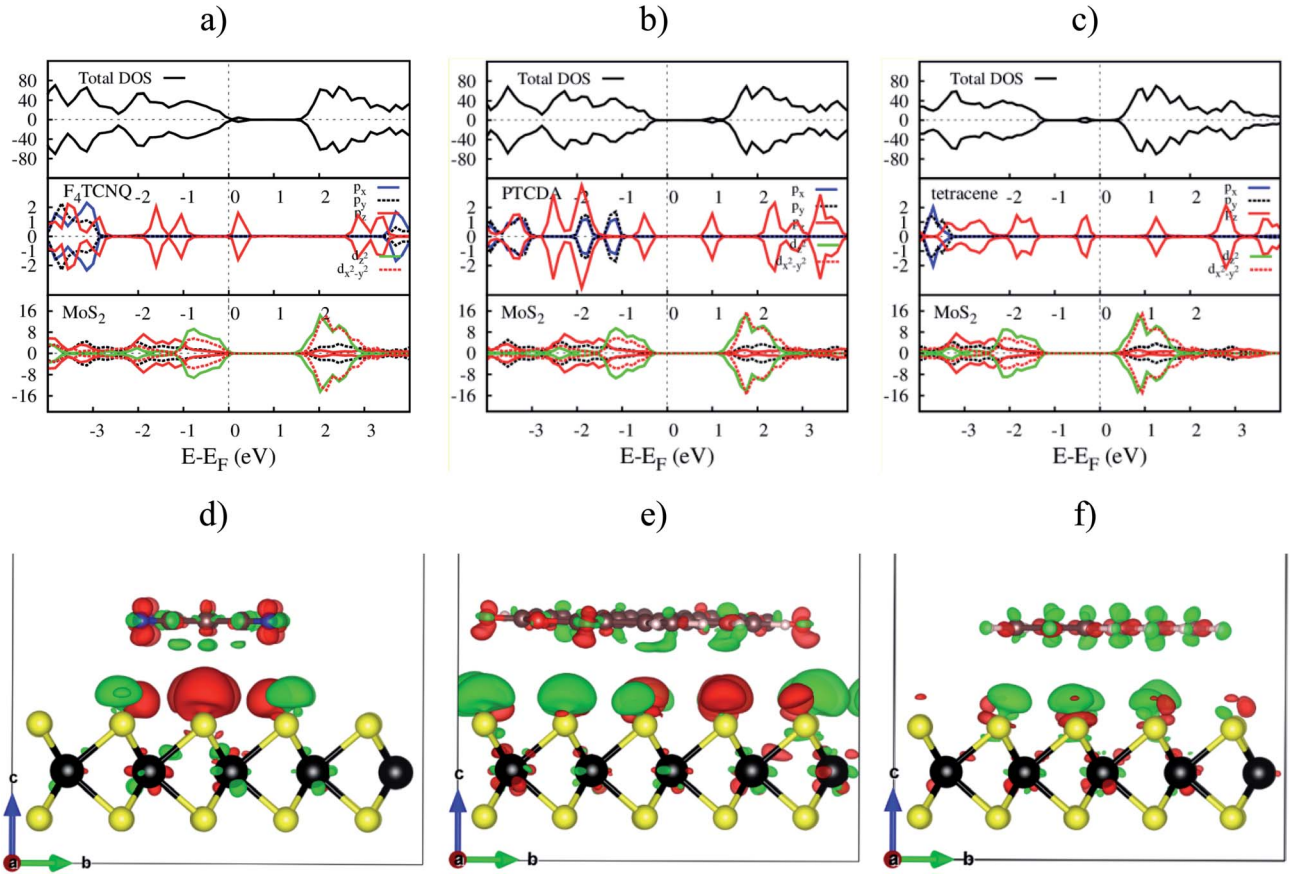

Fig. 7 The upper panel is the total and orbital-projected DOS. The bottom panel is the charge density difference at zero pressure. From left to right is for MoS_2/F_4TCNQ, MoS_2/PTCDA, and MoS_2/tetracene, respectively. Occupied and unoccupied states are presented in red and green in that order.

PTCDA, while the charge donation distributes more on tetracene. This result is in agreement with the above analysis about the Bader charge.

Fig. 8 shows the response of the total electronic density of states toward the influence of pressure. The p-type doping F_4TCNQ and PTCDA shift the valence band maximum of MoS_2 upward, while the n-type doping tetracene moves the conduction band minimum of MoS_2 downward near to the Fermi level. The variation of the position of the valence band maximum and conduction band minimum leads to modifying the bandgap of the systems.

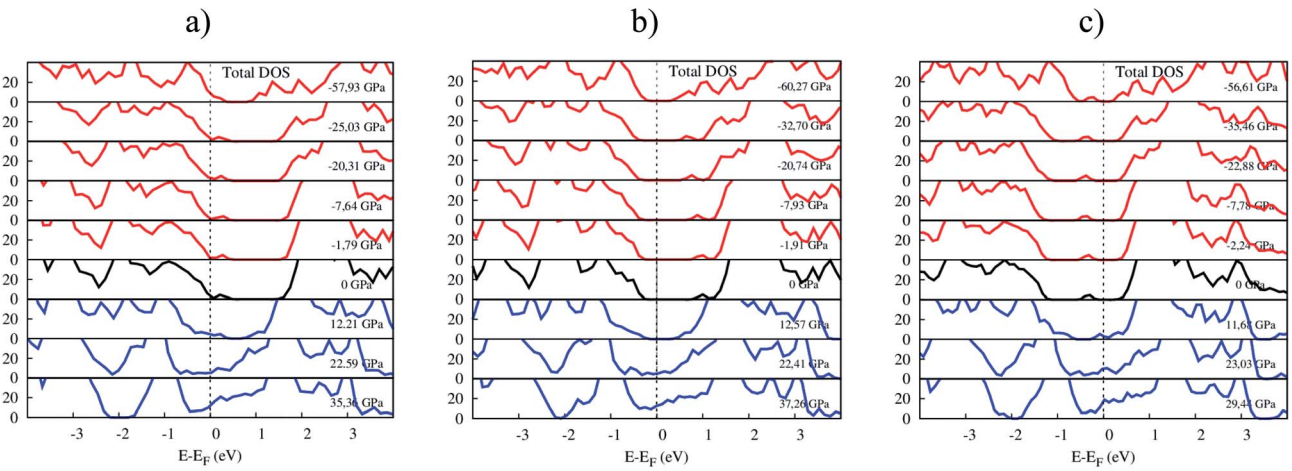

Fig. 8 The total DOS of (a) MoS_2/F_4TCNQ, (b) MoS_2/PTCDA, and (c) MoS_2/tetracene under pressure.

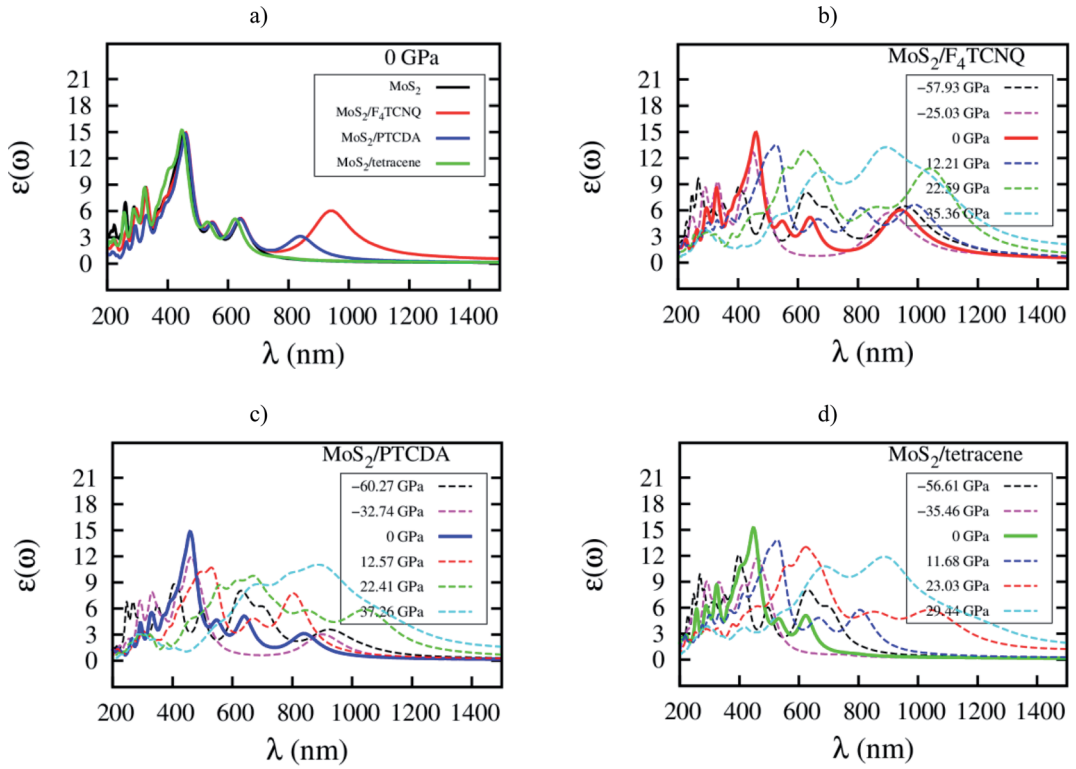

Fig. 9 Imaginary part of dielectric function $\varepsilon(\omega)$ *versus* wavelength λ for (a) the systems at zero pressure, (b) MoS_2/F_4TCNQ, (c) MoS_2/PTCDA, and (d) MoS_2/tetracene under pressure.

3.3. Optical properties

Here, we elucidate the influences of the organic molecular adsorption on the optical properties of the monolayer MoS_2. The imaginary part of the frequency-dependent dielectric function of the MoS_2, MoS_2/F_4TCNQ, MoS_2/PTCDA, and MoS_2/tetracene in the independent-particle approximation including local field effects is presented in Fig. 9. After that, optical parameters as listed in Table 6 can be obtained in two steps: (1) determining the wavelength λ and the intensity $\varepsilon(\omega)$ at the maximum peak of the dielectric function, check Fig. 9, (2) calculating the corresponding photon energy $E_p = \hbar c/\lambda$. At zero pressure, we found in Fig. 9a that the optical spectrum of the MoS_2/F_4TCNQ, MoS_2/PTCDA, and MoS_2/tetracene systems has the maximum peak at almost the same position as that of the monolayer MoS_2, which is at about 450 nm. The result indicates that these systems can emit and absorb blue light.[29,37] The optical spectrum of the MoS_2/tetracene has almost the same

Table 6 The wavelength and dielectric function at the maximum intensity of optical spectrum

MoS_2 (ref. 33)	P (GPa)	**−56.18**	**−32.44**	**0**	**10.13**	**24.95**	**41.14**
	E_p (eV)[a]	4.66	2.60	2.73	2.39	2.00	1.42
	λ (nm)	266	477	453	521	621	873
	$\varepsilon(\omega)$	11.06	11.58	14.88	13.36	13.18	12.06
MoS_2/F_4TCNQ	P (GPa)	**−57.93**	**−25.03**	**0**	**12.21**	**22.59**	**35.36**
	E_p (eV)[a]	4.62	2.75	2.69	2.36	1.99	1.38
	λ (nm)	268	451	461	526	624	896
	$\varepsilon(\omega)$	9.65	12.66	14.95	13.54	12.92	13.22
MoS_2/PTCDA	P (GPa)	**−60.27**	**−32.74**	**0**	**12.57**	**22.41**	**37.26**
	E_p (eV)[a]	3.06	2.67	2.71	2.34	1.86	1.39
	λ (nm)	405	463	458	529	668	889
	$\varepsilon(\omega)$	8.82	11.95	14.82	10.72	9.76	11.05
MoS_2/tetracene	P (GPa)	**−56.61**	**−35.46**	**0**	**11.68**	**23.03**	**29.44**
	E_p (eV)[a]	3.11	2.69	2.77	2.36	1.99	1.40
	λ (nm)	398	461	447	526	623	886
	$\varepsilon(\omega)$	12.11	11.72	15.21	13.85	13.03	11.90

[a] $E_p = hc/\lambda$ is the photon energy, λ is the photon wavelength, h is Planck constant, and c is the speed of light in vacuum.

behavior as the monolayer MoS_2 with a little modification at short wavelengths around 300 nm. Contrastingly, the MoS_2/F_4TCNQ and MoS_2/PTCDA exhibits an additional peak at 950 and 850 nm, respectively. It is necessary to remind that the MoS_2/F_4TCNQ and MoS_2/PTCDA are p-type, while the MoS_2/tetracene is an n-type semiconductor. The behavior of the optical spectrum of the MoS_2/tetracene was found to be similar to that of the n-type doping of MoS_2 with PEI.[33] Therefore, the auxiliary peak at a longer wavelength was only found for the monolayer MoS_2 with the p-type doping.[5] Furthermore, as shown in Fig. 9b–d, the intensity of the main optical peak at non-zero pressures was suppressed compared to that at 0 GPa.

4. Conclusion

This work investigated the effects of the organic molecular adsorption on the physical properties of the monolayer MoS_2 by the DFT calculations. The results have proved that the adsorption of F_4TCNQ, PTCDA, and tetracene on MoS_2 is physisorption. The organic molecular adsorption reduces the direct bandgap of the monolayer MoS_2 to 0.36, 1.43, and 0.72 eV, respectively. The main cause is due to the emergence of the new energy level at the conduction band minimum for MoS_2/F_4TCNQ and MoS_2/PTCDA, and at the valence band maximum for MoS_2/tetracene, by the p_z orbitals of the adsorbates. Under pressure, the bandgap of the MoS_2/F_4TCNQ, MoS_2/PTCDA, and MoS_2/tetracene systems reaches the maximum value of 0.36, 1.43, and 0.87 eV, respectively. Whilst, it becomes 0 eV implying the transition to the metal at the tensile pressure of 22.59, 22.41, and 23.03 GPa in that order. The adsorption of tetracene changes the optical peak structure of the monolayer MoS_2 at the ultraviolet region around 300 nm; however, the F_4TCNQ and PTCDA adsorption generate an auxiliary peak at the long wavelengths.

Conflicts of interest

There are no conflicts of interest to declare.

Acknowledgements

This research is funded by Ho Chi Minh City University of Technology (HCMUT), VNU-HCM, under grant number BK-SDH-2021-1680479.

References

1 B. Radisavljevic, A. Radenovic, J. Brivio, V. Giacometti and A. Kis, Single-layer MoS_2 transistors, *Nat. Nanotechnol.*, 2011, **6**, 147–150.
2 A. Splendiani, L. Sun, Y. Zhang, T. Li, J. Kim, C.-Y. Chim, G. Galli and F. Wang, Emerging Photoluminescence in Monolayer MoS_2, *Nano Lett.*, 2010, **10**, 1271.
3 K. F. Mak, C. Lee, J. Hone, J. Shan and T. F. Heinz, Atomically thin MoS_2: a new direct-gap semiconductor, *Phys. Rev. Lett.*, 2010, **105**, 136805.
4 M. Chhowalla, H. S. Shin, G. Eda, L.-J. Li, K. P. Loh and H. Zhang, The chemistry of two-dimensional layered transition metal dichalcogenide nanosheets, *Nat. Chem.*, 2013, **5**(4), 263–275.
5 Y. Jing, X. Tan, Z. Zhou and P. Shen, Tuning electronic and optical properties of MoS_2 monolayer *via* molecular charge transfer, *J. Mater. Chem. A*, 2014, **2**, 16892–16897.
6 W. Chen, S. Chen, D. C. Qi, X. Y. Gao and A. T. Wee, Surface transfer p-type doping of epitaxial graphene, *J. Am. Chem. Soc.*, 2007, **129**(34), 10418–10422.
7 Y. Du, H. Liu, A. T. Neal, M. Si and P. D. Ye, Molecular Doping of Multilayer MoS_2 Field-Effect Transistors: Reduction in Sheet and Contact Resistances, *IEEE Electron Device Lett.*, 2013, 0741–3106.
8 H. Huang, Y. Huang, S. Wang, M. Zhu, H. Xie, L. Zhang, X. Zheng, Q. Xie, D. Niu and Y. Gao, Van Der Waals Heterostructures between Small Organic Molecules and Layered Substrates, *Crystals*, 2016, **6**, 113.
9 Q. Huy Thi, H. Kim, J. Zhao and T. Hue Ly, Coating two-dimensional MoS_2 with polymer creates a corrosive non-uniform interface, *npj 2D Mater. Appl.*, 2018, **2**, 34.
10 H. Pinto, R. Jones, J. P. Goss and P. R. Briddon, p-type doping of graphene with F_4TCNQ, *J. Phys.: Condens. Matter*, 2009, **21**, 402001.
11 S. Mouri, Y. Miyauchi and K. Matsuda, Tunable Photoluminescence of Monolayer MoS_2 *via* Chemical Doping, *Nano Lett.*, 2013, **13**(12), 5944–5948.
12 P. Hu, J. Ye, X. He, K. Du, K. K. Zhang, X. Wang, Q. Xiong, Z. Liu, H. Jiang and C. Kloc, Control of Radiative Exciton Recombination by Charge Transfer Induced Surface Dipoles in MoS_2 and WS_2 Monolayers, *Sci. Rep.*, 2016, **6**, 24105.
13 J. Wang, Z. Ji, G. Yang, X. Chuai, F. Liu, Z. Zhou, C. Lu, W. Wei, X. Shi, J. Niu, L. Wang, H. Wang, J. Chen, N. Lu, C. Jiang, L. Li and M. Liu, Charge Transfer within the F_4TCNQ-MoS_2 van der Waals Interface: Toward Electrical Properties Tuning and Gas Sensing Application, *Adv. Funct. Mater.*, 2018, **28**(51), 1806244.
14 T. Ogawa, K. Kuwamoto, S. Isoda, T. Kobayashi and N. Karl, 3,4:9,10-Perylenetetracarboxylic dianhydride (PTCDA) by electron crystallography, *Acta Crystallogr., Sect. B: Struct. Sci.*, 1999, **55**, 123–130.
15 S. Heutz, A. J. Ferguson, G. Rumbles and T. S. Jones, Morphology, structure and photophysics of thin films of perylene-3,4,9,10-tetracarboxylic dianhydride, *Org. Electron.*, 2002, **3**, 119–127.
16 Y. Han, W. Ning, H. Du, J. Yang, N. Wang, L. Cao, F. Li, F. Zhang, F. Xu and M. Tian, Preparation, Optical and Electrical Properties of PTCDA Nanostructures, *Nanoscale*, 2015, **7**, 17116–17121.
17 M. R. Habib, H. Li, Y. Kong, T. Liang, S. M. Obaidulla, S. Xie, S. Wang, X. Ma, H. Su and M. Xu, Tunable Photoluminescence in van der Waals Heterojunction Built from MoS_2 Monolayer and PTCDA Organic Semiconductor, *Nanoscale*, 2018, **10**, 16107–16115.
18 S. Wang, C. Chen, Z. Yu, Y. He, X. Chen, Q. Wan, Y. Shi, D. W. Zhang, H. Zhou, X. Wang and P. Zhou, A MoS_2/

PTCDA Hybrid Heterojunction Synapse with Efficient Photoelectric Dual Modulation and Versatility, *Adv. Mater.*, 2018, **31**(3), 1806227.

19 L. Daukiya, J. Seibel and S. D. Feyter, Chemical modification of 2D materials using molecules and assemblies of molecules, *Adv. Phys.*, 2019, **4**(1), 1625723.

20 R. W. I. de Boer, T. M. Klapwijk and A. F. Morpurgo, Field-effect transistors on tetracene single crystals, *Appl. Phys. Lett.*, 2003, **83**, 4345.

21 H. J. Park, C.-J. Park, J. Y. Kim, M. S. Kim, J. Kim and J. Joo, Hybrid Characteristics of MoS_2 Monolayer with Organic Semiconducting Tetracene and Application to Anti-Ambipolar Field Effect Transistor, *ACS Appl. Mater. Interfaces*, 2018, **10**(38), 32556–32566.

22 G. Kresse and J. Hafner, *Ab initio* molecular dynamics for open-shell transition metals, *Phys. Rev. B: Condens. Matter Mater. Phys.*, 1993, **48**, 13115–13118.

23 G. Kresse and J. Hafner, *Ab initio* molecular-dynamics simulation of the liquid-metal–amorphous-semiconductor transition in germanium, *Phys. Rev. B: Condens. Matter Mater. Phys.*, 1994, **49**, 14251–14269.

24 G. Kresse and J. Furthmuller, Efficient iterative schemes for *ab initio* total-energy calculations using a plane-wave basis set, *Phys. Rev. B: Condens. Matter Mater. Phys.*, 1996, **54**, 11169–11186.

25 P. E. Blochl, Projector augmented-wave method, *Phys. Rev. B: Condens. Matter Mater. Phys.*, 1994, **50**, 17953.

26 G. Kresse and J. Joubert, From ultrasoft pseudopotentials to the projector augmented-wave method, *Phys. Rev. B: Condens. Matter Mater. Phys.*, 1999, **59**, 1758.

27 J. P. Perdew, J. A. Chevary, S. H. Vosko, K. A. Jackson, M. R. Pederson, D. J. Singh and C. Fiolhais, Atoms, molecules, solids, and surfaces: applications of the generalized gradient approximation for exchange and correlation, *Phys. Rev. B: Condens. Matter Mater. Phys.*, 1992, **46**, 6671.

28 J. P. Perdew, K. Burke and M. Ernzerhof, Generalized Gradient Approximation Made Simple, *Phys. Rev. Lett.*, 1996, **77**, 3865.

29 Y. Li, Y.-L. Li, C. M. Araujo, W. Luo and R. Ahuja, Single-layer MoS_2 as an efficient photocatalyst, *Catal.: Sci. Technol.*, 2013, **3**, 2214.

30 H. J. Monkhorst and J. D. Pack, Special points for Brillouin zone integrations, *Phys. Rev. B: Solid State*, 1976, **13**, 5188–5192.

31 J. Shang, L. Zhang, X. Cheng and F. Zhai, Pressure induced effects on the electronic and optical properties of MoS_2, *Solid State Commun.*, 2015, **219**, 33–38.

32 L. J. Kong, G. H. Liu and L. Qiang, Electronic and optical properties of O-doped monolayer MoS_2, *Comput. Mater. Sci.*, 2016, **111**, 416–423.

33 O. K. Le, V. Chihaia, M.-P. Pham-Ho and D. N. Son, Electronic and optical properties of monolayer MoS_2 under the influence of polyethyleneimine adsorption and pressure, *RSC Adv.*, 2020, **10**, 4201–4210.

34 M. M. Ugeda, A. J. Bradley, *et al.*, Giant bandgap renormalization and excitonic effects in a monolayer transition metal dichalcogenide semiconductor, *Nat. Mater.*, 2014, **13**, 1091–1095.

35 X. Cheng, Y. Li, J. Shang, C. Hu, Y. Ren, M. Liu and Z. Qi, Thickness-dependent phase transition and optical behavior of MoS_2 films under high pressure, *Nano Res.*, 2018, **11**, 855–863.

36 V. K. Dien, O. K. Le, V. Chihaia, M. P. Pham-Ho and D. N. Son, Monolayer transition-metal dichalcogenides with polyethyleneimine adsorption, *J. Comput. Electron.*, 2021, DOI: 10.1007/s10825-020-01630-2.

37 Z. Yin, H. Li, H. Li, L. Jiang, Y. Shi, Y. Sun, G. Lu, Q. Zhang, X. Chen and H. Zhang, Single-Layer MoS_2 Phototransistors, *ACS Nano*, 2011, **6**, 74–80.